

Experimental verification of a constitutive model of fibre composite with hyperelastic matrix

Svitlana Fedorova¹, Tomáš Lasota², Jiří Burša³, Pavel Skácel⁴

Abstract: The paper compares computational simulations of tension and bending tests on the basis of an anisotropic hyperelastic constitutive model with experimental results. The tested specimens are made of rubber with a single family of textile fibres under different angles. As our previous studies have shown substantial discrepancies between computational and experimental results, now we used textile fibres (with zero bending stiffness) instead of steel wires and the matrix was made of rubber with a very limited Mullins effect to eliminate the possible causes of errors. The results have shown that the simulations correspond well to the experiments.

Keywords: Anisotropy; Hyperelasticity; Fibre composite; Finite strain

1. Introduction

Fibre composites with elastomer matrix are widely used as elements of pneumatic and hydraulic structures. Carbon-black filled rubber is mostly used as matrix of these composites, and steel wires or ropes, textile and other fibres are used as their reinforcement. While material properties of most fibre composites are linear elastic and the theory of the linear elasticity is well known and widely used for any types of anisotropic materials under small strain conditions, large strains induced in elastomers make the stress-strain analyses much more difficult and not yet fully managed. Although first applicable isotropic hyperelastic models were formulated in forties and fifties of the last century [1,2], their broader practical application has not started before nineties, when the power of computers has enabled to solve more complex non-linear problems. However, there is still a lack of criteria for assessment of the risk of failure of isotropic elastomers [3,4].

The situation is even worse with fibre composites with elastomer matrix showing large strains [5]. First anisotropic hyperelastic models have been published in the last decade [6,7] and implemented into commercial finite element packages only several years ago. There is no experience with their practical application, with

¹ Ing. Svitlana Fedorova; Institute of Solid Mechanics, Mechatronics and Biomechanics, Fac. of Mech. Engineering, Brno University of Technology; Technická 2896/2, 616 69 Brno, Czech Republic; sf13@ukr.net

² Ing. Tomáš Lasota; dtto; tlasota@seznam.cz

³ Prof. Ing. Jiří Burša, Ph.D.; dtto; bursa@fme.vutbr.cz

⁴ Ing. Pavel Skácel, Ph.D.; dtto; skacy@email.cz

identification of their parameters, so that even their use in research is rather exceptional. The paper presents results of our attempts to simulate basic mechanical tests of these fibre composites using FEM and their experimental verification.

2. Experimental methods

Uniaxial tension tests of composite specimens with a rubber matrix and single family of textile fibres in the middle layer of the specimen were carried out. Four groups of specimens with different declination of fibres were tested: 0° , 30° , 45° , 90° . All the specimens had dimensions approximately $110 \times 22 \times 2.5$ mm and diameter of the fibres 0.8 mm. All the specimens were loaded in cycles with different amplitudes to evaluate Mullins effect [8]. The upper amplitude of total elongation of the specimen is nearly 20 mm, with the exception of 0° declination (longitudinal fibres), where the elongation had to be several times lower because of the much higher stiffness of the specimen. Tension tests were realized using universal testing machine ZWICK Z020-TND. Elongation in the middle region of the specimen was recorded by extensometers (Fig. 1); the distance between extensometer levers was 20 mm.

A particular feature of the tests with specimens with fibre declination is that dimensions of specimens strongly affect results. Stress-strain curve would be different for the specimens with the same angle of declination but different width or length.

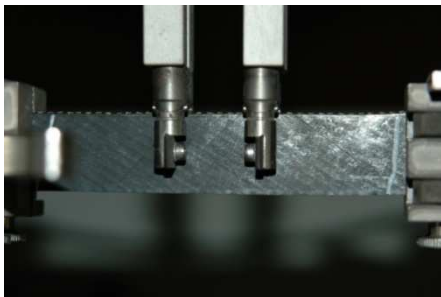


Fig. 1. Tension test of fibre composite with rubber matrix



Fig. 2. Bending test of fibre composite with rubber matrix

Bending tests were realized also with the ZWICK testing machine as a three point bending. For the tests specimens with the following fibre declination were used: 0° , 45° , 90° . Also pure rubber specimens were tested. Specimens had dimensions approximately $60 \times 20 \times 2.5$ mm and diameter of the fibres approximately 0.8 mm. The distance between supports was 50 mm.

During the test each specimen was placed in the test preparation and pushed against its middle part (Fig. 2). The dependency between the force and the middle deflection was recorded.

Experiments on pure rubber were carried out as well in order to determine material constants for hyperelastic potential of the matrix. They included uniaxial and equibiaxial tension of rubber specimens. As the parameters of the textile fibres are rather uncertain and were not known, their stiffness was identified on the basis of the tension test with fibres in longitudinal direction.

3. Methods of computational simulations

Material of the specimens shows large strains and incompressibility (due to rubber) and a substantial anisotropy (due to fibres).

Rubber matrix of the specimen is characterized by large reversible deformations. Its behaviour is approximated as so called hyperelastic. Constitutive modelling in this case is based on the concept of strain energy density function (strain energy potential). Stress-strain relations are derived from this potential. Generally strain energy potential for isotropic hyperelastic material is based on the strain invariants.

For rubber-like materials, a phenomenological polynomial form of strain energy potential is widely used. It is based on the first and second strain invariants and is given by the following formula:

$$W = \sum_{i+j=1}^3 c_{ij} (I_1 - 3)^i (I_2 - 3)^j + \sum_{k=1}^N \frac{1}{d} (J - 1)^{2k}, \quad (1)$$

where $J = \lambda_1 \lambda_2 \lambda_3$ - volume ratio; c_{ij}, d - material constants.

In our case, given that in all tests local tensile strains do not exceed 40%, the simplest Neo-Hooke model can be used for rubber matrix:

$$W = \frac{\mu}{2} (I_1 - 3) + \frac{1}{d} (J - 3)^2. \quad (2)$$

To model the behaviour of the given specimens, we need to account for the material anisotropy. As the specimens have one family of fibres, they have a single preferred direction. In this direction the stiffness of the material is defined by the stiffness of fibres. The fibres are uniformly distributed throughout the middle layer of the specimen (with approximately constant spacing). It enables us to use continuum approach for constitutive modelling of specimens. It takes into account contribution of both constituents: fibres and rubber.

Specimens for bending simulations were modelled using sandwich structure with the middle layer being anisotropic hyperelastic and two others being isotropic hyperelastic. Specimens for tension simulations (with the exception of 0° case) were modelled as homogeneous, using anisotropic hyperelastic material model. It has been proved that for uniaxial tension both of the models give the same results for all fibre declinations except for 0°.

Strain energy potential used for anisotropic hyperelastic materials consists of isotropic and anisotropic parts. The anisotropic part includes strain invariant I_4 :

$$I_4 = \bar{a}C\bar{a}, \quad (3)$$

where \bar{a} is unit vector characterising the preferred direction in the undeformed configuration (see [6] or [7] for details) and C is right Cauchy-Green deformation tensor, given by squared stretch ratios in the principal coordinate system:

$$C = \begin{pmatrix} \lambda_1^2 & 0 & 0 \\ 0 & \lambda_2^2 & 0 \\ 0 & 0 & \lambda_3^2 \end{pmatrix}. \quad (4)$$

If XY coordinate plain coincides with the specimen's middle plain, the fibre vector has coordinates $(\cos \alpha, \sin \alpha, 0)$ where α defines the fibre declination angle. Accordingly, invariant I_4 (representing stretch of fibres) is given by:

$$I_4 = \lambda_1^2 \cos^2 \alpha + \lambda_2^2 \sin^2 \alpha. \quad (5)$$

Anisotropic hyperelastic strain energy potential can be given by polynomial form:

$$W = \sum_{i=1}^3 a_i (I_1 - 3)^i + \sum_{j=1}^3 b_j (I_2 - 3)^j + \sum_{k=2}^6 c_k (I_4 - 1)^k. \quad (6)$$

Constants for potential (6) are being determined from the characteristics of constituents (rubber and fibres).

Isotropic part of potential (6) can be set in the form of Neo-Hooke model for an incompressible rubber:

$$\varphi_i = \frac{\mu}{2} (I_1 - 3). \quad (7)$$

Material constant for rubber was determined on the basis of the stress –strain curves obtained from two sets of experiments: uniaxial tension and equibiaxial tension of rubber specimens. Approximation of response curves was performed employing the least squares method.

The anisotropic part of potential (6) reflects characteristics of composite in the preferred direction. It was set as follows:

$$\varphi_a = c_2 (I_4 - 1)^2. \quad (8)$$

Consequently, potential (6) acquires the form

$$W = \frac{\mu}{2} (I_1 - 3) + c_2 (I_4 - 1)^2. \quad (9)$$

One of the difficulties in constitutive modelling of reinforced elastomers is due to the presence of Mullins effect in rubber [8]. Mullins effect is generally known as softening of stress response during repeated loading. At this stage of research we

don't have any continuous hyperelastic model at our disposal in FE analyses, which would account for both Mullins effect and anisotropy.

Also it is not possible to eliminate Mullins effect by preconditioning of the composite specimens, since rubber in the composite experiences non uniform stress and strain states and cannot be preconditioned with the same strain amplitude throughout the specimen.

Our previous studies of specimens with steel fibres [9] have shown substantial discrepancies between the computational and experimental results. There were two main reasons: first, the anisotropic hyperelastic constitutive model we used could not account for the bending stiffness of steel fibres and second, the presence of Mullins effect in rubber. Therefore in the present study we use textile fibres (with zero bending stiffness) and rubber with low Mullins effect, thus eliminating possible causes of errors.

Specific type of rubber was chosen on the basis of preliminary uniaxial tension tests with different rubbers used typically for production of car tyres. From the loading and unloading curves it is clear that Mullins effect does not exceed 10 % of engineering stress for this type of rubber. Consequently, its influence on the results was neglected in this study.

4. Results

In this section results of experiments and the corresponding computational simulations are presented.

4.1. Uniaxial tension

The figures below present results of uniaxial tension tests and their simulations. In all the figures the abscissa represents the elongation of the middle part of the specimen with original length of 20 mm. Tests were carried out with four groups of specimens: two specimens with 0° fibre declination, per three specimens with 30° and 45° fibre declination and five specimens with the declination of 0°. Material constants used in part of potential (9) were set: $\mu = 1,2$ MPa, $c_2 = 60$ MPa. While the simulations have been done only under monotonous loading (without unloading), all the experiments were carried out in several cycles so that hysteresis and Mullins effect are evident.

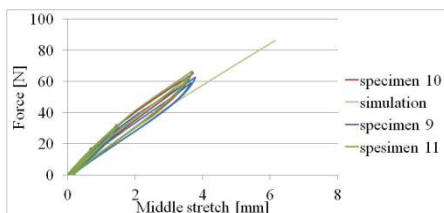


Fig. 3. Results of the tension test and its simulation for 30° declination of fibres.

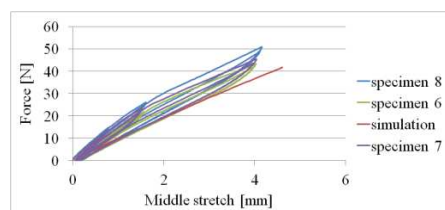


Fig. 4. Results of the tension test and its simulation for 45° declination of fibres.

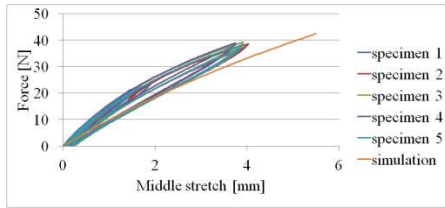


Fig. 5. Results of the tension test and its simulation for 90° declination of fibres.

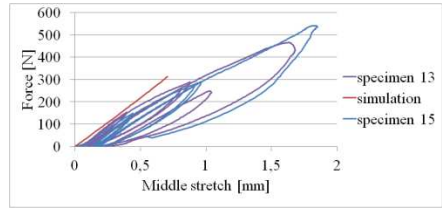


Fig. 6. Results of the tension test and its simulation for 0° declination of fibres.

4.2. Results of bending simulations

The figures below present results of bending tests and their simulations. Tests were carried out with four groups of three specimens each: for 0° , 45° and 90° declination of fibres and for pure rubber. The same material parameters were set as for the tension test simulations.

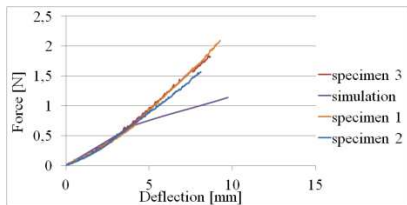


Fig. 7. Results of the bending test and its simulation for 0° declination of fibres.

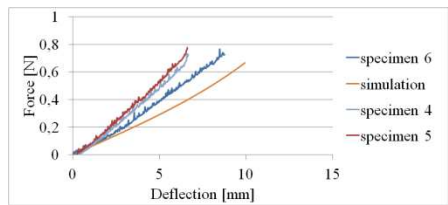


Fig. 8. Results of the bending test and its simulation for 45° declination of fibres.

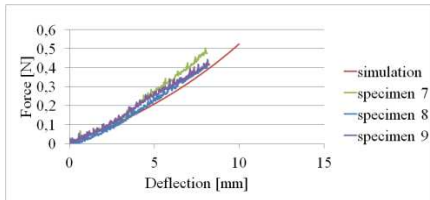


Fig. 9. Results of the bending test and its simulation for 90° declination of fibres.

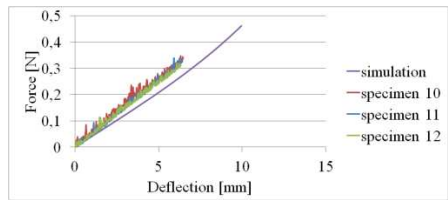


Fig. 10. Results of the bending test and its simulation. Specimens made of pure rubber.

4.3. Assessment of fibre declination influence

Table 1 presents dependency between fibre declination and force for the given displacement $u = 0.5$ mm for uniaxial tension. Table 2 presents dependency between fibre declination and force for the given deflection $v = 4$ mm for bending. Results are taken from the numerical simulations of the tests.

Table 1. Influence of fibre declination angle for uniaxial tension tests

Declination angle, deg.	Force, N
0	216,42
30	12,23
45	5,03
90	4,77

Table 2. Influence of fibre declination angle for bending tests

Declination angle, deg.	Force, N
0	0,98
45	0,23
90	0,16

5. Discussion

As it was shown in [9], the bimaterial model (which includes models of geometry of both matrix and fibres) in the case of tension load can be successfully replaced with the unimaterial one. It enables us a substantial reduction of computational time.

It is evident from Fig. 3-6 that simulations are in a good agreement with the tests for all fibre declinations. The case of 0° fibre declination needs a particular explanation. The specimen was modelled as a three-layer sandwich with upper and bottom rubber layers (using isotropic hyperelastic potential) and a fibre-reinforced middle layer (using potential (9)). The specimen elongation during the experiment is mainly due to the shear in rubber layers between the jaws. The aim of numerical simulation was to determine material constant c_2 representing the stiffness of fibres in (9). The potential (9) was employed in computational model; accordingly, constant c_2 was varied until an acceptable agreement between the simulation and the experimental response was reached.

Nevertheless, in the modelling of tension tests on specimens in which fibres clamped on both ends are absent (due to the geometry of specimen and angle of fibre declination) the value of c_2 can be set very high, insuring inextensibility of fibres. The stiffness of the fibres is much larger than that of the rubber, so that only a negligible fibre elongation occurs.

An opposite situation occurs with bending tests simulations; the value of c_2 shows a great influence on the results. Therefore the results of simulation in Fig.6 were taken into account and the modified value of c_2 was used to insure correct constitutive modelling of bending tests. Specimens for bending tests were not preconditioned and local tensile strain in simulation was lower than 6%. With that in mind we further employ the model which shows good agreement with initial test curve in the range of smaller deformations as shown in Fig.6.

In simulation of bending tests with 0° declination of fibres, there is a turning point in the deflection-force curve (Fig. 7). The same problem occurred with steel fibres [9] if their angle was small (less than 15°). As the position of the turning point

depends on the stiffness of the fibres we can hypothesise that the effect can be caused by buckling of fibres in the compressed part of the model. However, this problem requires a detailed investigation in future.

The results in Fig. 8 show a rather higher discrepancy between the simulation and the experimental loading curves. It can be explained by the inaccuracy of experiments, during which some initial torsion of the specimens was present and thus the deflection changed throughout the specimen width.

The simulation curves in Fig. 9-10 correspond well to the tests. As it was expected, the stiffening effect of the fibres with 90° fibre declination is negligible and results for these specimens are very close to those obtained for pure rubber.

6. Conclusion

It was verified that anisotropic hyperelastic constitutive model (in polynomial form) is able to simulate credibly results of tension and bending tests of fibre composites showing large strains under the following conditions: elastomer matrix shows negligible Mullins effect; bending stiffness of fibres is negligible.

There are still some numerical problems in simulations of bending tests with longitudinal fibres which need to be investigated in greater detail.

References

- [1] Mooney M., "A Theory of Large Elastic Deformation", *Journal of Applied Physics*, **6**, pp. 582-592 (1940). 0021-8979.
- [2] Rivlin R.S., "*Philos. Trans. R. Soc. London, A*" pp. 243,251 (1951).1364-503X.
- [3] Legorju-jago K., Bathias C., "Fatigue Initiation and Propagation in Natural and Synthetic Rubbers ", *International Journal of Fatigue*, **24**, pp. 85-92 (2002). 0142-1123.
- [4] Rivlin R. S., Thomas A. G., "Rupture of rubber. Part 1. Characteristic energy for tearing", *Journal of Polymer Science*, **10**, pp. 291-318 (1953). 0887-624X.
- [5] Janíček P., Burša J., "Experimental and computational modelling of adhesion strength in composite materials", in *Proceedings of Seventh International Conference Damage and Fracture Mechanics VII*, Kihei, USA, 2002, pp. 403-411. 1-85312-926-7/1462-6055.
- [6] Spencer A.J.M., "Constitutive theory for strongly anisotropic solids", in *Continuum Theory of the Mechanics of Fibre-Reinforced Composites, CISM Courses and Lectures No. 282*, Spencer A.J.M., ed. (International Centre for Mechanical Sciences, Springer-Verlag, Wien, 1984), pp. 1-32.
- [7] Holzapfel G.A., Gasser T.C., Ogdan R.W., "A new constitutive framework for arterial wall mechanics and a comparative study of material models", *Journal of Elasticity*, **61**, pp.1-47 (2000). 0374-3535.
- [8] Mullins L., "Effect of stretching on the properties of rubber", *Journal of rubber research*, **16**, pp. 275-289 (1947). 1511-1768.
- [9] Lasota T., Burša J. "Simulation of mechanical tests of composite material using anisotropic hyperelastic constitutive models", *Engineering Mechanics*, **18**(1), pp. 23-32 (2011). 1802-1484.